Electronic Supplementary Material (ESI) for Organic & Biomolecular Chemistry.
This journal is © The Royal Society of Chemistry 2022

Electronic Supplementary Information

The Role of Acetylated Cyclooxygenase-2 in the Biosynthesis of Resolvin Precursors Derived from Eicosapentaenoic Acid

Anna Cebrián-Prats[1], Alexandre Pinto [2], Àngels González-Lafont[1,3], Pedro A. Fernandes*[2], and José M. Lluch[1,3]*

[1]Departament de Química, Universitat Autònoma de Barcelona, 08193 Bellaterra, Barcelona, Spain

[2]LAQV-Requimte, Faculty of Sciences, University of Porto, Rua do Campo Alegre S/N, Porto, Portugal.

[3]Institut de Biotecnologia i de Biomedicina (IBB), Universitat Autònoma de Barcelona, 08193 Bellaterra, Barcelona, Spain

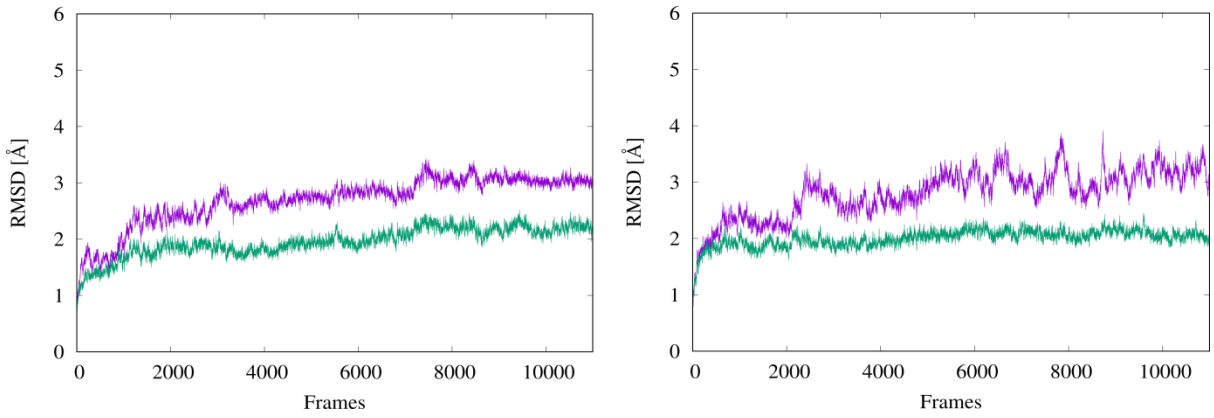

Figure S1. RMSD of the protein α-carbons (purple line) and RMSD excluding the residues of the N-terminal domain (green line) in the COX-2/EPA Michaelis complex. RMSDs are referenced to the first structure of the 100 ns MD simulation. On the right, the RMSD with Tyr385-O˙ in the COX-2 pocket is shown, and on the left, the RMSD with Tyr385 is represented. One frame has been taken each 10 ps.

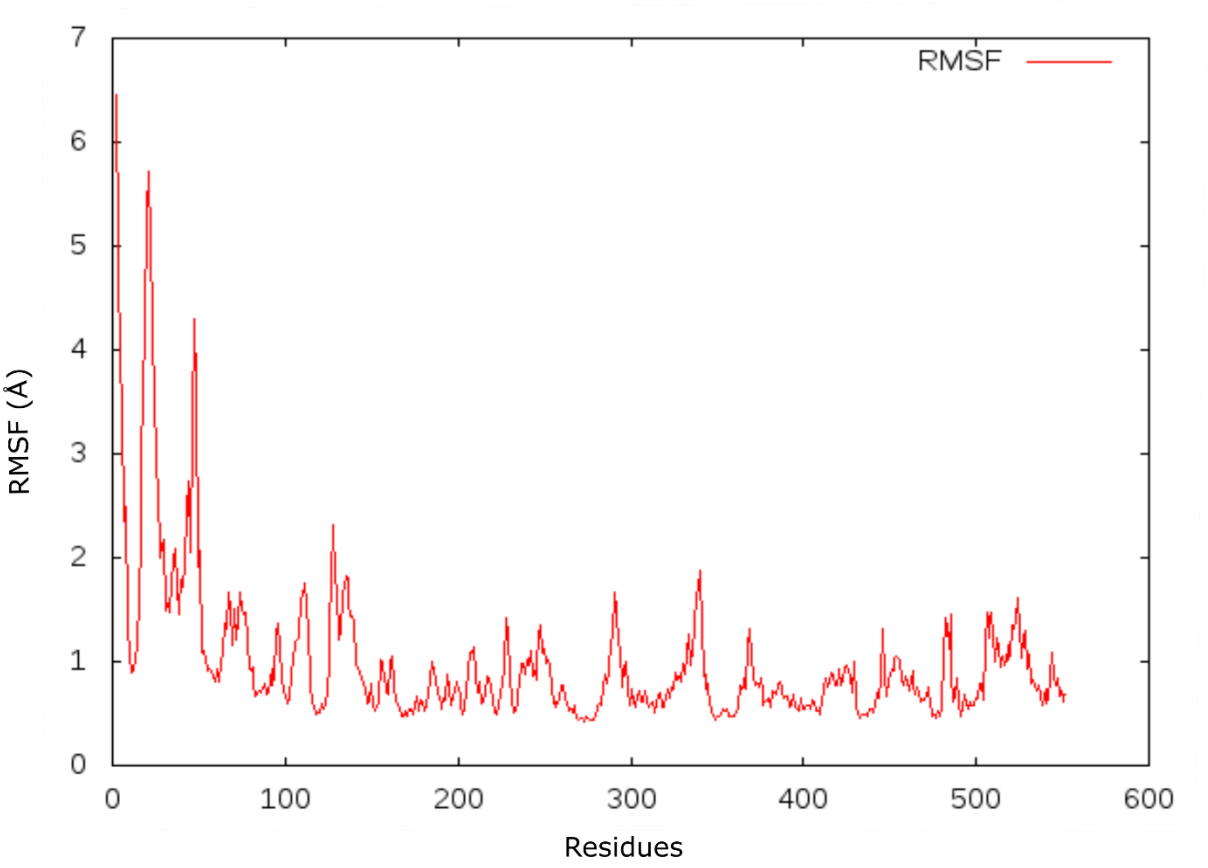

Figure S2. RMSF per residue of the protein for the MD simulation of the COX-2/EPA Michaelis complex.

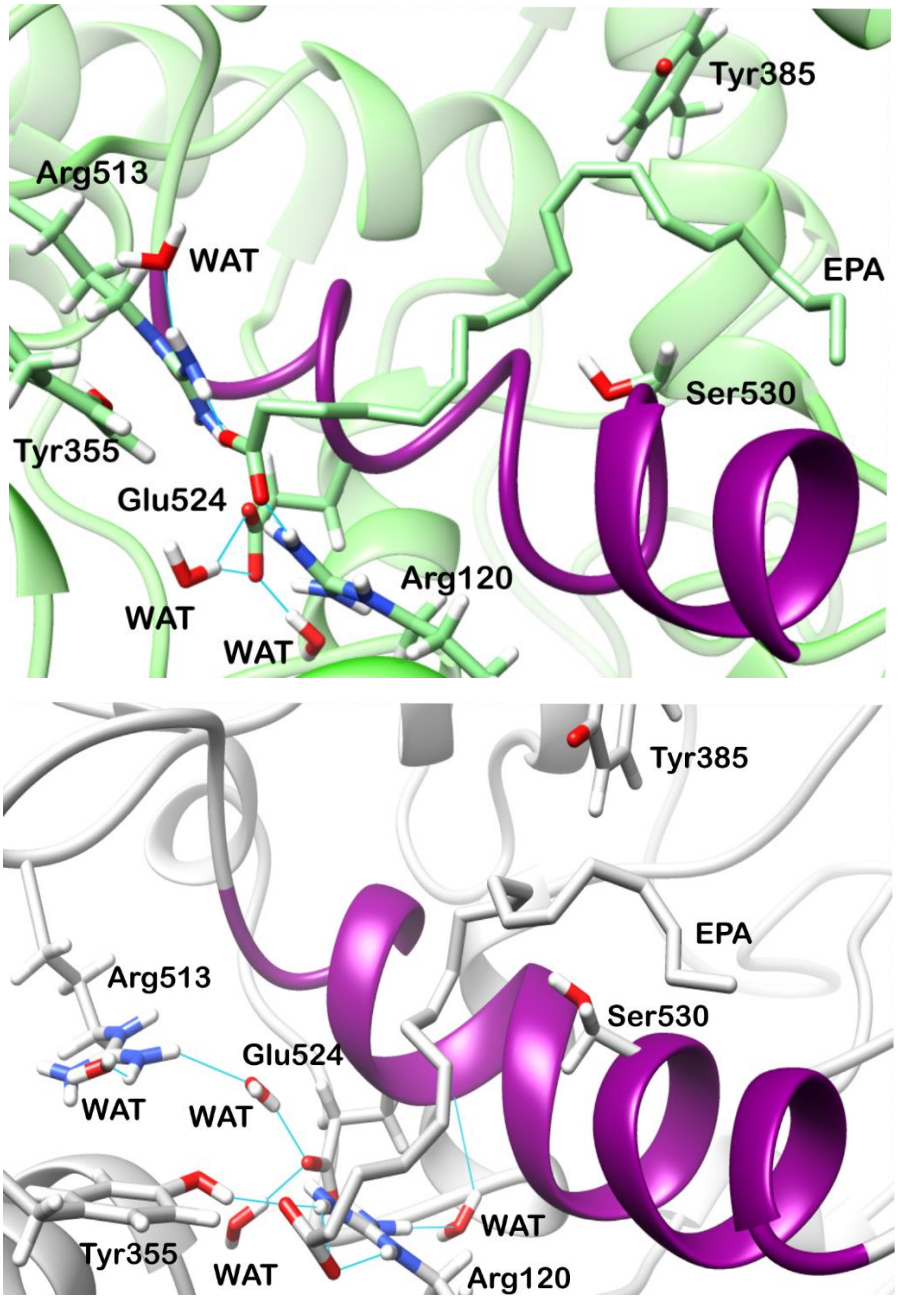

Figure S3 Binding modes of the EPA substrate inside the hydrophobic groove of COX-2 in the presence of the Tyr385-O· radical for the pre-catalytic snapshots IV (in green), and V (in gray) of the H_{13proR} and H_{16proR} abstractions, respectively. The main hydrogen bonds at the pocket entrance are shown.

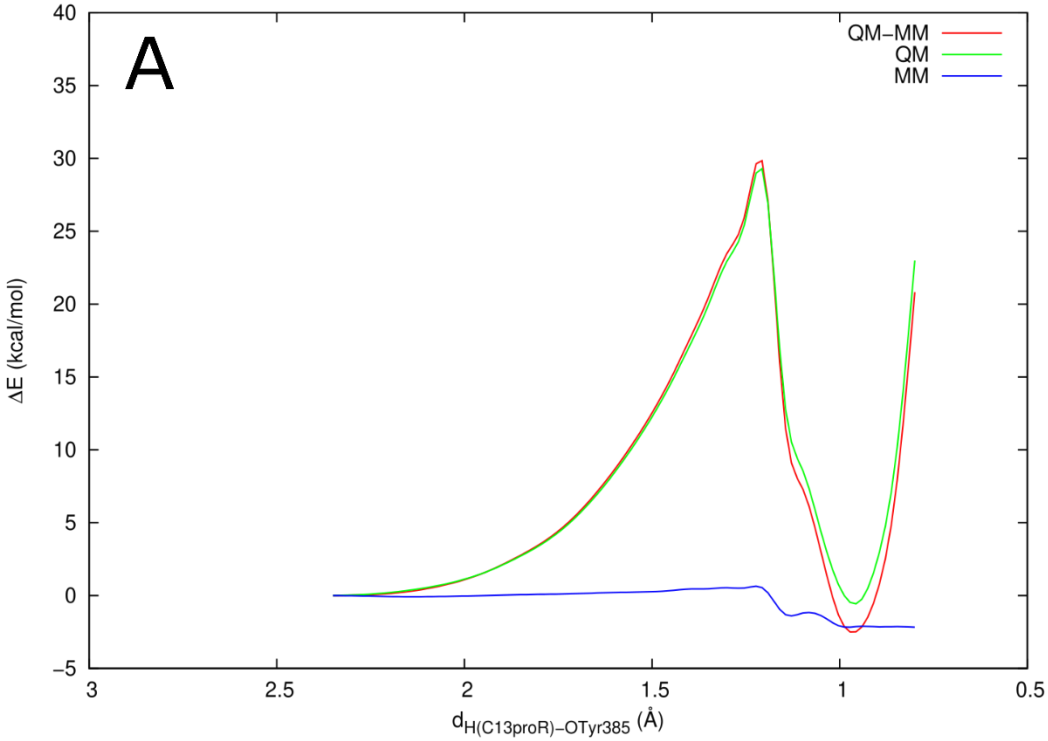
A
QM–MM
QM
MM
ΔE (kcal/mol)
40
35
30
25
20
15
10
5
0
−5
3
2.5
2
1.5
1
0.5
$d_{H(C13proR)-OTyr385}$ (Å)

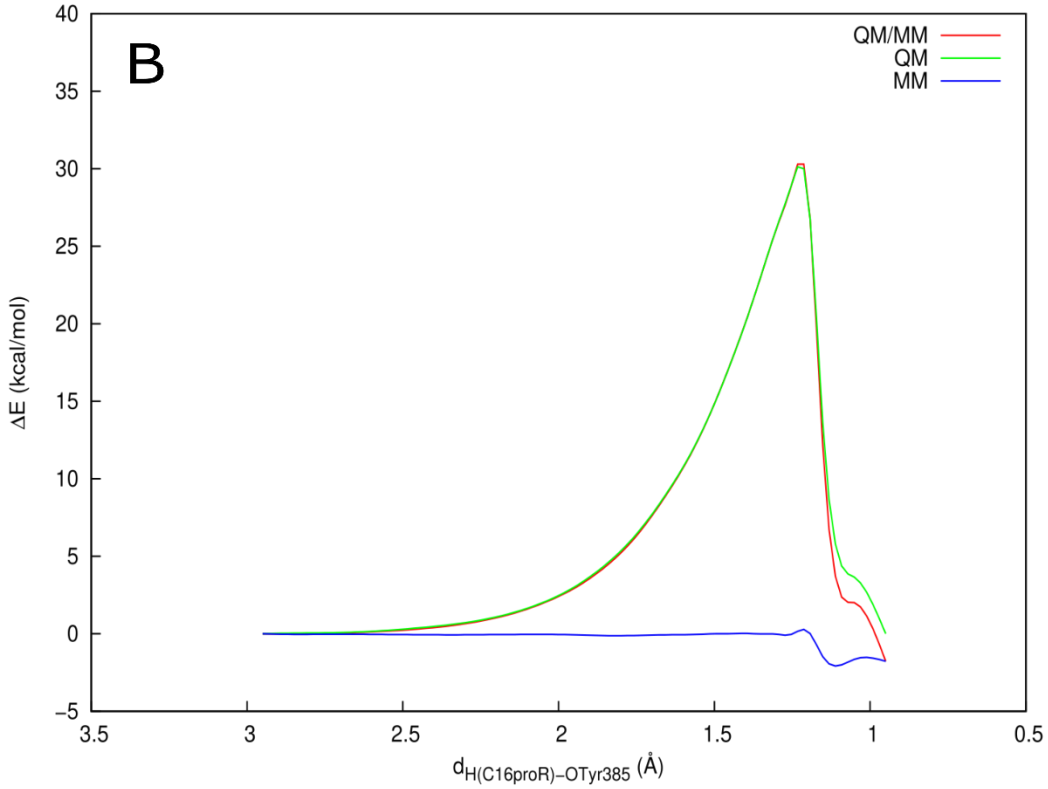
B
QM/MM
QM
MM
ΔE (kcal/mol)
40
35
30
25
20
15
10
5
0
−5
3.5
3
2.5
2
1.5
1
0.5
$d_{H(C16proR)-OTyr385}$ (Å)

Figure S4. B3LYP/6-31G(d,p):AMBER potential energy profiles for A) snapshot II (H_{13proR} abstraction), and B) snapshot V (H_{16proR} abstraction) in the COX-2/EPA complex, showing the QM and MM contributions to the total QM/MM energy along the H-abstraction reaction coordinate.

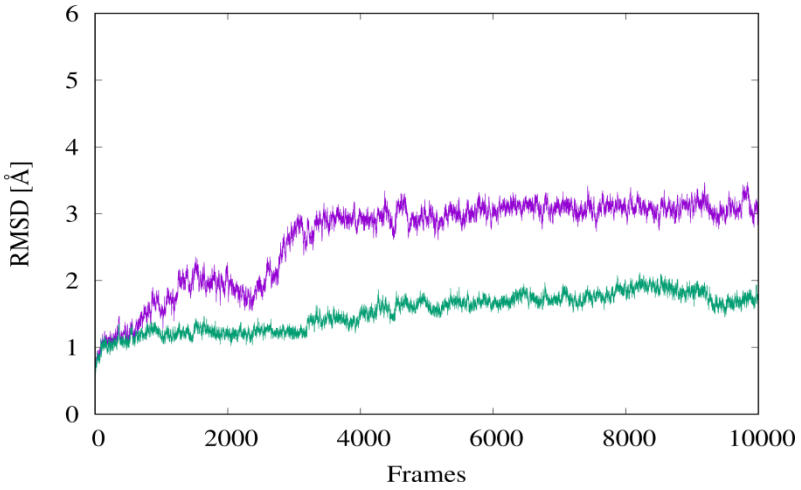

Figure S5. RMSD of the protein α-carbons (purple line) and RMSD excluding the residues of the N-terminal domain (green line). RMSDs are referenced to the first structure of the 100 ns MD simulation of the aspirin-acetylated COX-2/EPA complex, including Tyr385-$O^{\cdot}$ into the active site. One frame has been taken each 10 ps.

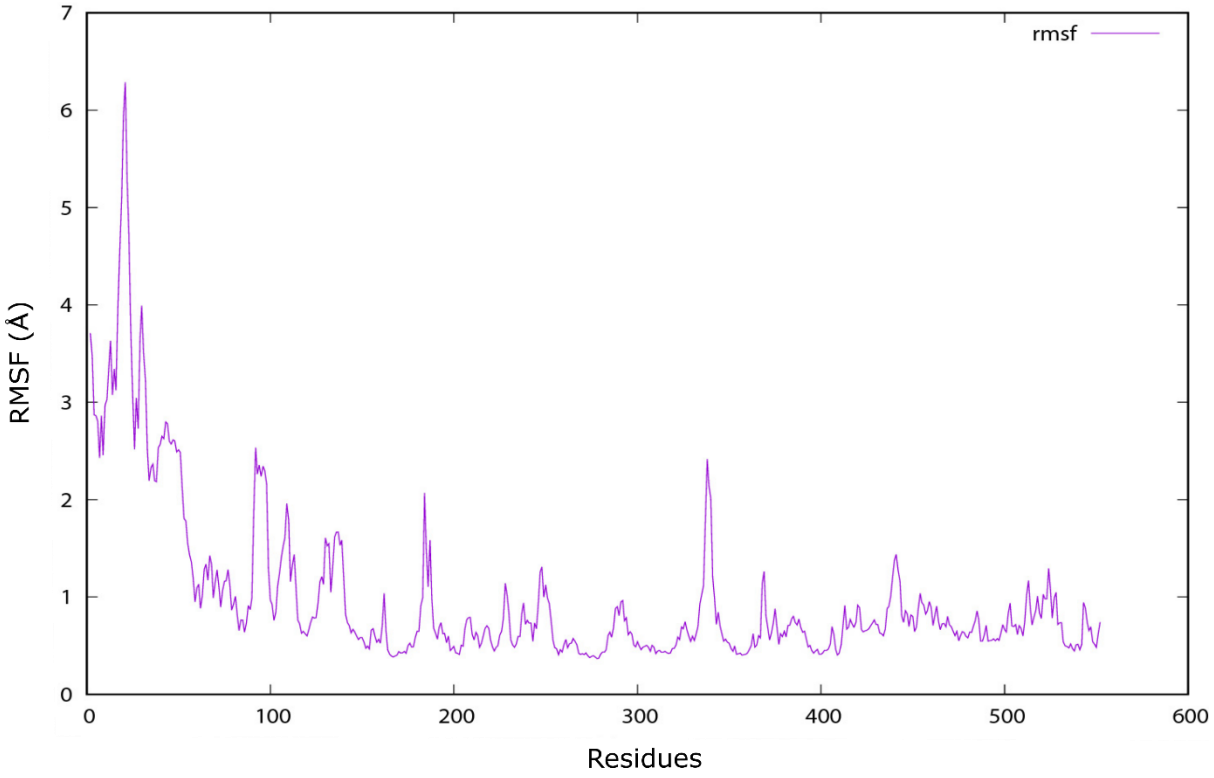

Figure S6. RMSF per residue of the protein for the MD simulation of the aspirin-acetylated COX-2/EPA Michaelis complex.

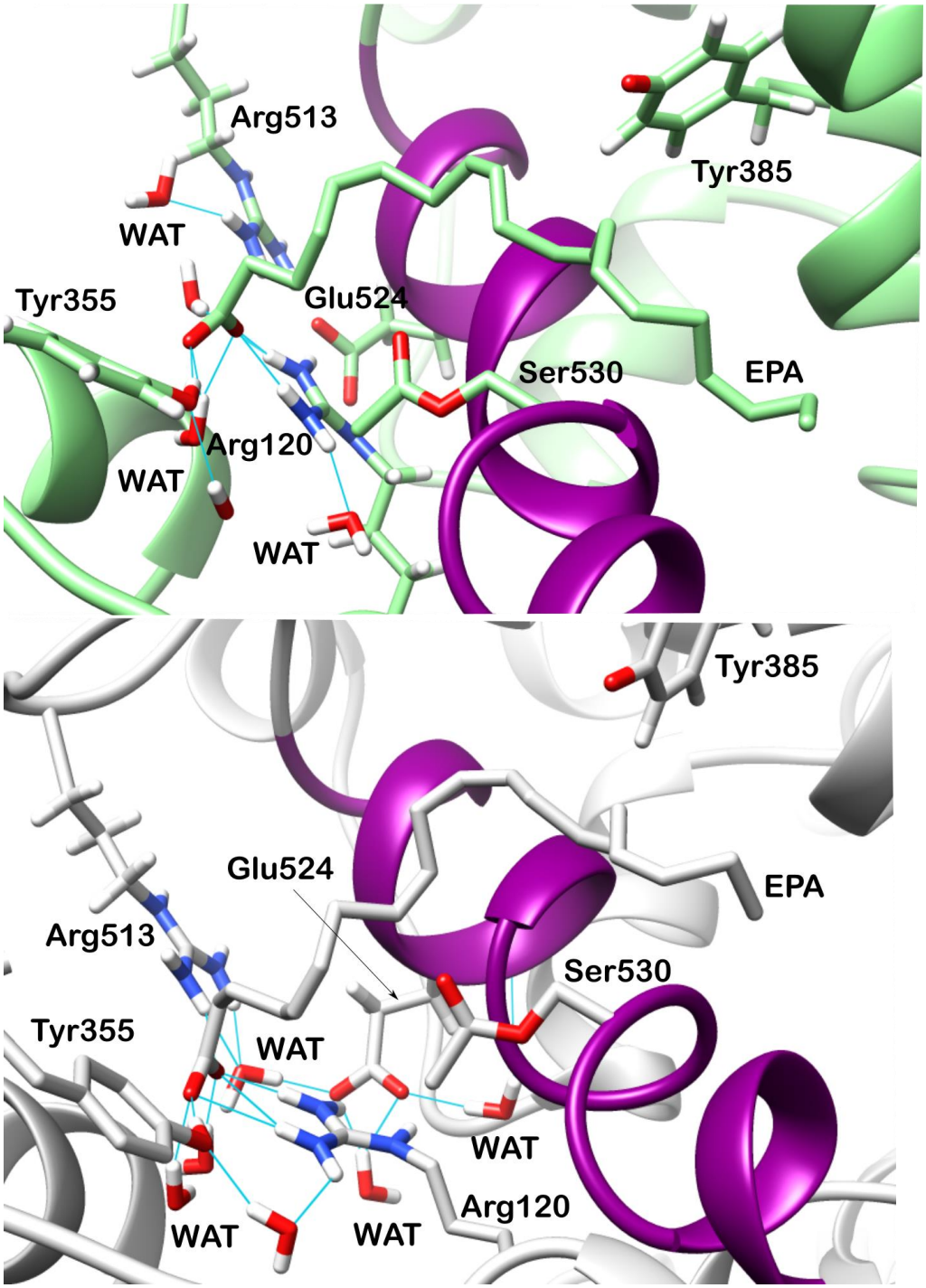

Figure S7. Binding modes of the EPA substrate inside the hydrophobic groove of aspirin-acetylated COX-2 in the presence of the Tyr385-O· radical for the pre-catalytic snapshots IV (H_{13proS} abstraction) in green, and snapshot VIII (H_{16proS} abstraction) in gray, showing the main hydrogen bonds at the pocket entrance.

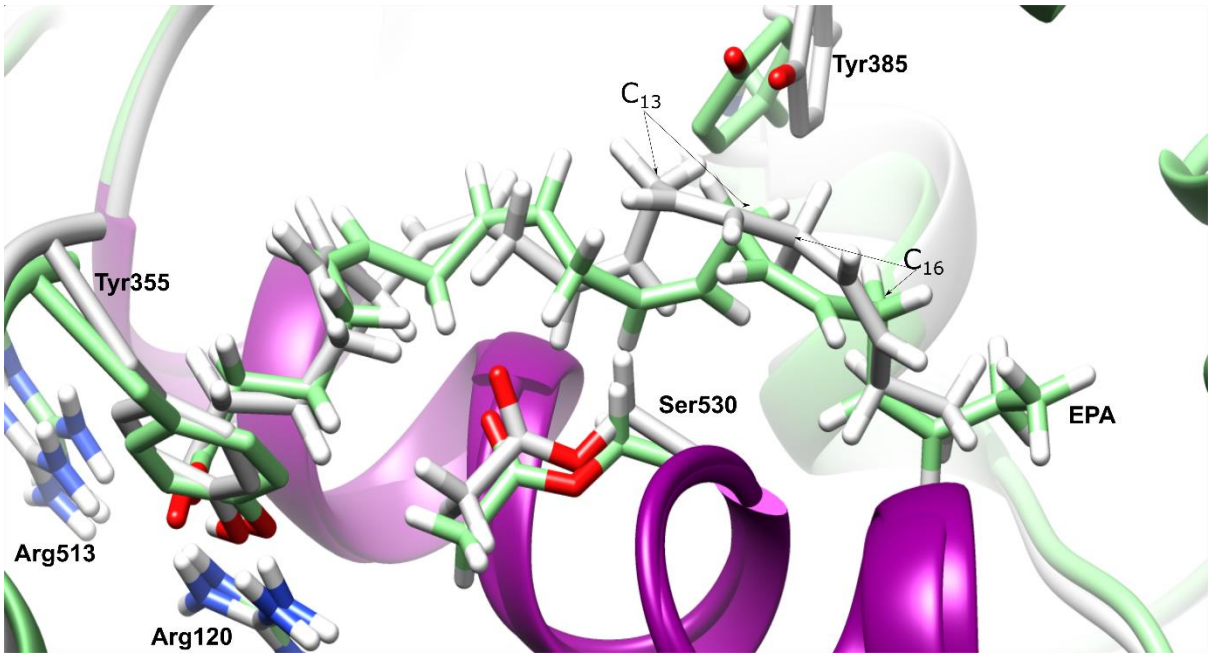

Figure S8 Overlay between snapshots IV (H_{13proS}) in green and VII (H_{16proS}) in gray inside the hydrophobic groove of aspirin-acetylated COX-2 in the presence of the Tyr385-O· radical.

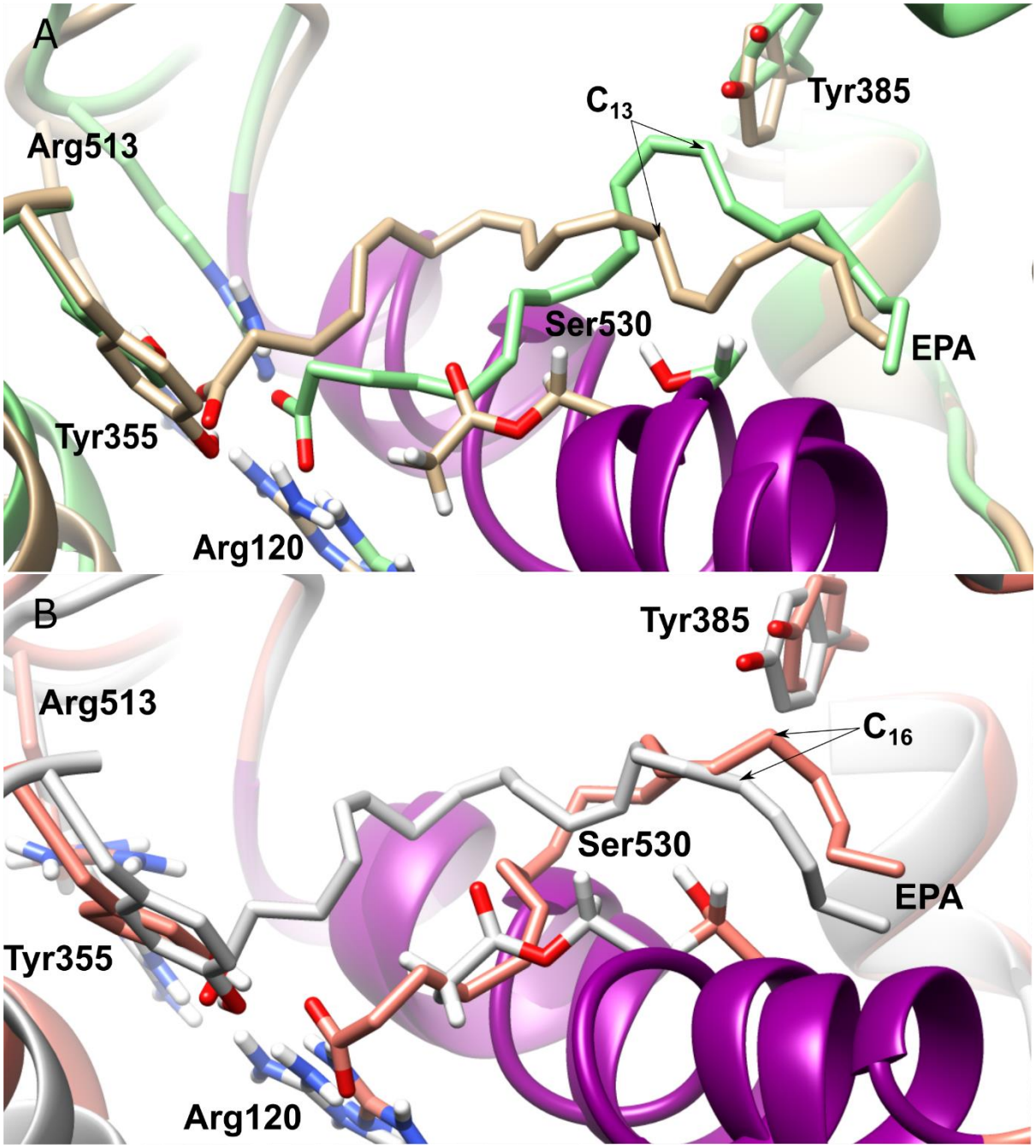

Figure S9. A) Overlay between EPA binding modes of snapshots IV (H_{13proR}) green colour and I (H_{13proS}) tan colour inside the hydrophobic groove of COX-2 and aspirin-acetylated COX-2, respectively, in the presence of the Tyr385-O· radical; B) Overlay between EPA binding modes of snapshots V (H_{16proR}) salmon colour and VII (H_{16proS}) gray colour inside the hydrophobic groove of COX-2 and aspirin-acetylated COX-2, respectively, in the presence of the Tyr385-O· radical. Hydrogens of EPA are not shown for clarity.

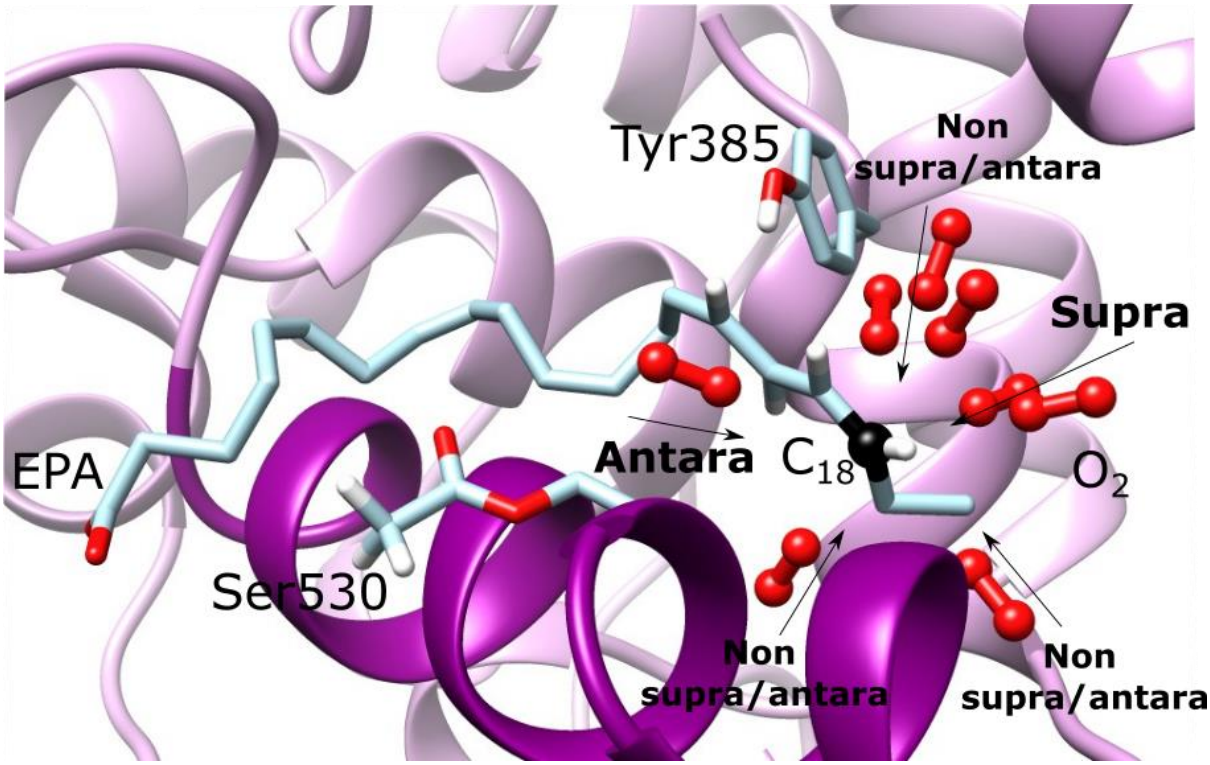

Figure S10. The 8 starting points for the case of the O_2 addition to C_{18} in snapshot VII in the aspirin-acetylated COX-2/EPA complex**.**

Table S1. Average H_{13proX}-OTyr385 and H_{16proX}-OTyr385 distances (in Å) along the two MD simulations of the COX-2/EPA Michaelis complex.

MD	**H_{13proR}**		**H_{13proS}**		**H_{16proR}**		**H_{16proS}**	
Time (ns)	0-55	55-100	0-55	55-100	0-55	55-100	0-55	55-100
Tyr385-OH	3.27	3.93	4.08	5.04	4.35	6.31	5.88	6.45
Time (ns)	0-55	55-100	0-55	55-100	0-55	55-100	0-30	30-100
Tyr385-O$^{\cdot}$	3.01	5.43	4.37	5.16	3.58	4.38	5.14	4.43

Table S2. Main hydrogen bonds at the entrance of the hydrophobic groove for representative pre-catalytic snapshots of COX-2/EPA (IV in Figure S2) and aspirin-acetylated COX-2/EPA (IV and VIII in Figure S5) complexes in the presence of the Tyr385-O· radical. The hydrogen bonds for a representative snapshot of the COX-2/AA complex are also given for the sake of comparison. The hydrogen bonds between the enzyme and the corresponding fatty acid are shadowed. The distances are given in Å.

COX-2: EPA (H_{13proR})

Hydrogen Donor		Acceptor		D-H…A
ARG120	HE	EPA	O1	1.95
ARG120	HH11	WAT	O	1.84
ARG120	HH21	EPA	O1	2.30
ARG120	HH21	EPA	O2	2.06
TYR355	HH	EPA	O2	1.73
ARG513	H	WAT	O	1.89
ARG513	HE	WAT	O	1.89
ARG513	HH11	WAT	O	1.87
ARG513	HH21	WAT	O	2.38
ARG513	HH21	WAT	O	2.43
ARG513	HH22	WAT	O	2.20
WAT	H1	TYR355	OH	2.22
WAT	H2	TYR355	OH	2.01
WAT	H1	EPA	O2	1.66
WAT	H2	EPA	O1	2.05
WAT	H2	GLU524	OE2	1.80
WAT	H2	GLU524	OE2	1.85

COX-2:AA

Hydrogen Donor		Acceptor		D-H…A
ARG120	HE	AA	O2	2.03
ARG120	HH11	WAT	O	1.87
ARG120	HH21	AA	O1	2.08
ARG120	HH21	AA	O2	2.08
TYR355	HH	WAT	O	1.73
ARG513	HH12	AA	O1	1.92
ARG513	HH11	WAT	O	1.88
ARG513	HH22	AA	O1	1.92
ARG513	HH21	WAT	O	2.13
SER530	HG	WAT	O	2.03
WAT	H1	AA	O1	1.61
WAT	H2	TYR355	OH	2.44

WAT	H1	AA	O2	1.78
WAT	H1	GLY533	O	2.30
WAT	H1	GLU524	OE2	2.03
WAT	H1	GLU524	OE1	1.66
WAT	H2	GLU524	OE1	1.74
WAT	H2	GLU524	O	2.48
WAT	H2	TYR355	O	1.97
WAT	H1	ARG120	O	1.69

Acetylated COX-2 : EPA (H_{13proS})

Hydrogen Donor		Acceptor		D-H…A
ARG120	H	WAT	O	2.08
ARG120	HH12	EPA	O1	1.99
ARG120	HH11	WAT	O	2.15
ARG120	HH22	EPA	O1	2.00
ARG120	HH22	WAT	O	2.50
TYR355	HH	EPA	O2	1.65
ARG513	H	WAT	O	1,91
ARG513	HH11	WAT	O	2.11
LEU531	H	WAT	O	2.05
WAT	H1	GLU524	O	1,95
WAT	H2	WAT	O	1,91
WAT	H1	EPA	O1	2.00
WAT	H1	EPA	O2	1.99
WAT	H1	TYR355	OH	2.29
WAT	H1	GLU524	OE1	1.74
WAT	H1	TYR355	O	1.85
WAT	H2	GLY533	O	1.89
WAT	H1	GLU524	OE1	1.77
WAT	H1	EPA	O1	1.63

Acetylated COX-2 : EPA (H_{16proS})

Hydrogen Donor		Acceptor		D-H…A
ARG120	H	WAT	O	2.02
ARG120	HH12	EPA	O1	2.60
ARG120	HH12	EPA	O2	2.50
ARG120	HH11	WAT	O	2.64
ARG120	HH22	EPA	O1	1.92
TYR355	HH	EPA	O2	1.75
ARG513	H	WAT	O	2.36
ARG513	HH12	EPA	O1	2.39
ARG513	HH12	WAT	O	2.31
ARG513	HH22	WAT	O	1.90
LEU531	H	WAT	O	2.08
WAT	H1	TYR355	O	1.82

WAT	H2	GLU524	OE1	1.97
WAT	H2	GLU524	OE1	1.76
WAT	H2	GLU524	OE2	2,28
WAT	H2	EPA	O2	1.87
WAT	H1	GLY533	O	1.80
WAT	H2	EPA	O1	1.75
WAT	H1	GLU524	OE1	1.73
WAT	H2	TYR355	OH	2.02
WAT	H1	GLU524	O	2.07
WAT	H2	GLU524	OE2	1.94

Table S3. Potential energy barriers and reaction energies (in kcal/mol) obtained by means of QM/MM single point energy calculations at the M06/6-311+G(2d,2p):AMBER//B3LYP/6-31G(d,p):AMBER and M062X/6-311+G(2d,2p):AMBER//B3LYP/6-31G(d,p):AMBER levels corresponding to the H_{ZproR} hydrogen abstractions for those snapshots that have been able to reach the products in the COX-2/EPA complex.

Snapshots	**M06/6-311+G (2d,2p)**		**M062X/6-311+G (2d,2p)**	
H_{13proR}	$\Delta E^{\ddagger}$	ΔE	$\Delta E^{\ddagger}$	ΔE
I	28.6	-3.1	29.0	-3.2
II	28.7	-3.1	28.6	-3.1
IV	24.7	-9.6	24.6	-10.1
H_{16proR}	$\Delta E^{\ddagger}$	ΔE	$\Delta E^{\ddagger}$	ΔE
II	34.1	1.5	33.5	0.5
V	30.9	-3.3	30.2	-3.7

Table S4. The three interatomic distances (in Å) directly involved in the H_{13proR} and H_{16proR} abstractions at the B3LYP/6-31G(d,p):AMBER optimized reactant, transition state structure and product corresponding to the selected snapshots of the COX-2/EPA Michaelis complex. The potential energy barriers (in kcal/mol) are also included.[a]

Snapshots	$d(C\text{-}H)_R$	$d(H\text{-}O)_R$	$d(C\text{-}O)_R$	$d(C\text{-}H)_{TS}$	$d(H\text{-}O)_{TS}$	$d(C\text{-}O)_{TS}$	$d(C\text{-}H)_P$	$d(H\text{-}O)_P$	$d(C\text{-}O)_P$	$\Delta E^{\ddagger}$
H_{13proR}										
I	1.10	2.74	3.76	1.31	1.24	2.55	3.34	0.97	4.04	25.0
II	1.10	2.36	3.41	1.42	1.17	2.59	4.33	0.97	5.05	26.9
IV	1.10	2.83	3.46	1.36	1.21	2.53	2.55	0.97	3.27	22.3
H_{16proR}										
II	1.10	2.67	3.44	1.38	1.16	2.54	3.36	0.97	3.44	31.9
V	1.10	2.95	3.64	1.23	1.25	2.48	2.65	0.97	3.23	29.1

[a] H stands for the hydrogen atom to be transferred, C is the carbon atom to which H is attached, and O is the acceptor oxygen atom. R, TS and P stand for the reactant, transition state structure and product, respectively.

Table S5. Distances (Å) and dihedral angles (degrees) of the optimized radicals produced as products of the first H-abstraction step (either H_{13proR} or H_{16proR}) for snapshots I, II, IV, and V of the COX-2/EPA system.

H_{13proR}				
Snapshots	$d(C_{11}\text{-}C_{12})$	$d(C_{14}\text{-}C_{15})$	$Dihe(C_{11}\text{-}C_{12}\text{-}C_{13}\text{-}C_{14})$	$Dihe(C_{15}\text{-}C_{14}\text{-}C_{13}\text{-}C_{12})$
I	1.373	1.373	-175.26	23.08
II	1.372	1.375	-174.72	5.50
IV	1.373	1.369	-23.38	166.20
H_{16proR}				
Snapshots	$d(C_{14}\text{-}C_{15})$	$d(C_{17}\text{-}C_{18})$	$Dihe(C_{14}\text{-}C_{15}\text{-}C_{16}\text{-}C_{17})$	$Dihe(C_{18}\text{-}C_{17}\text{-}C_{16}\text{-}C_{15})$
II	1.371	1.372	-160.90	-9.77
V	1.370	1.373	-167.75	13.39

Table S6. Average H_{13proX}-OTyr385 and H_{16proX}-OTyr385 distances (in Å) along the MD simulation of the aspirin-acetylated COX-2/EPA Michaelis complex in the presence of the Tyr385-O· radical.

MD	**H_{13proR}**		**H_{13proS}**		**H_{16proR}**		**H_{16proS}**	
Time (ns)	0-40/ 80-100	40-80	0-25/ 35-100	25-35	0-40	40-100	0-5/ 40-100	5-40
Tyr385-O·	3.99/3.78	2.92	3.02 / 3.40	5.22	3.35	4.72	4.68/ 5.51	3.14

Table S7. The three interatomic distances (in Å) directly involved in the H_{13proS} and H_{16proS} abstractions at the optimized reactant, transition state structure and product corresponding to the selected snapshots of the aspirin-acetylated COX-2/EPA Michaelis complex. The potential energy barriers (in kcal/mol) are also included.[a]

Snapshots	**$d(C\text{-}H)_R$**	**$d(H\text{-}O)_R$**	**$d(C\text{-}O)_R$**	**$d(C\text{-}H)_{TS}$**	**$d(H\text{-}O)_{TS}$**	**$d(C\text{-}O)_{TS}$**	**$d(C\text{-}H)_P$**	**$d(H\text{-}O)_P$**	**$d(C\text{-}O)_P$**	**$\Delta E^{\ddagger}$**
H_{13proS}										
I	1.10	2.51	3.56	1.35	1.26	2.61	3.05	0.97	3.96	27.7
II	1.10	2.56	3.60	1.35	1.22	2.57	2.33	0.97	3.23	27.5
III	1.10	3.22	3.40	1.34	1.24	2.58	2.58	0.97	3.55	27.4
IV	1.10	2.62	3.31	1.34	1.23	2.58	3.06	0.97	3.99	27.0
V	1.10	2.86	3.62	1.36	1.22	2.58	2.39	0.97	3.30	24.3
H_{16proS}										
V	1.10	2.41	3.32	1.36	1.22	2.58	2.98	0.97	3.87	20.4
II	1.10	2.45	3.40	1.36	1.23	2.59	2.69	0.97	3.64	26.6
VI	1.10	2.22	3.24	1.37	1.22	2.59	3.07	0.97	3.95	26.9
VII	1.10	2.76	3.77	1.37	1.27	2.60	3.27	0.97	4.23	24.6
VIII	1.10	2.32	3.21	1.38	1.20	2.58	2.93	0.97	3.87	25.7

[a] H stands for the hydrogen atom to be transferred, C is the carbon atom to which H is attached, and O is the acceptor oxygen atom. R, TS and P stand for the reactant, transition state structure and product, respectively.

Table S8. Potential energy barriers and reaction energies (in kcal/mol) obtained by means of QM/MM single point energy calculations at the M06/6-311+G(2d,2p):AMBER//B3LYP/6-31G(d,p):AMBER and M062X/6-311+G(2d,2p):AMBER//B3LYP/6-31G(d,p):AMBER levels corresponding to the H_{13proS} and H_{16proS} hydrogen abstractions for those snapshots that have been able to reach the products in the aspirin-acetylated COX-2/EPA complex

Snapshots	**M06/6-311+G (2d,2p)**		**M062X/6-311+G (2d,2p)**	
H_{13proS}	$\Delta E^{\ddagger}$	ΔE	$\Delta E^{\ddagger}$	ΔE
I	30.7	-2.0	31.1	-2.2
II	29.6	6.3	29.0	5.3
III	29.2	-0.9	29.6	-0.9
IV	29.2	1.3	29.3	0.9
V	27.6	3.4	27.1	2.3
H_{16proS}	$\Delta E^{\ddagger}$	ΔE	$\Delta E^{\ddagger}$	ΔE
V	23.9	-4.4	23.6	-5.1
II	28.8	-0.1	28.9	-0.7
VI	31.3	1.1	31.8	1.1
VII	26.5	-13.6	26.5	-13.9
VIII	28.0	2.1	28.2	2.3

Table S9. Distances (Å) and dihedral angles (degrees) of the optimized radicals produced as products of the first H-abstraction step (either H_{13proS} or H_{16proS}) for the selected snapshots of the aspirin-acetylated COX-2/EPA system.

			H_{13proS}	
Snapshots	**$d(C_{11}-C_{12})$**	**$d(C_{14}-C_{15})$**	**$Dieh(C_{11}-C_{12}-C_{13}-C_{14})$**	**$Dieh(C_{15}-C_{14}-C_{13}-C_{12})$**
I	1.374	1.373	-172.68	-10.54
II	1.356	1.379	-46.80	-28.52
III	1.370	1.377	14.92	176.92
IV	1.372	1.375	13.86	176.02
V	1.365	1.371	-34.08	-35.00
			H_{16proS}	
Snapshots	**$d(C_{14}-C_{15})$**	**$d(C_{17}-C_{18})$**	**$Dieh(C_{14}-C_{15}-C_{16}-C_{17})$**	**$Dieh(C_{18}-C_{17}-C_{16}-C_{15})$**
V	1.374	1.373	14.75	-173.62
II	1.373	1.374	16.83	-175.76
VI	1.371	1.374	15.50	177.54
VII	1.375	1.371	179.63	174.53
VIII	1.373	1.375	14.43	-178.57

Table S10. Potential energy barriers and reaction energies (in kcal/mol) obtained by means of QM/MM single point energy calculations at the M06/6-311+G(2d,2p):AMBER//B3LYP/6-31G(d,p):AMBER level corresponding to the O_2 addition to C_{14} for all the pathways that have been able to reach the products for snapshot VII in the aspirin-acetylated COX-2/EPA complex. Antara and supra are the shortening word for antarafacial and suprafacial attack, respectively.

		M06/6-311+G (2d,2p)	
O_2 attack	**Stereochemistry C14 – Snap. VII**	$\Delta E^{\ddagger}$	ΔE
Antara	*R*	17.3	-14.8
Antara	*R*	9.0	-5.8
Antara	*R*	9.2	-6.2
Antara	*R*	16.8	4.0
Antara	*R*	8.9	-6.1
Supra	*S*	12.3	-1.5

Table S11. Potential energy barriers and reaction energies (in kcal/mol) obtained by means of QM/MM single point energy calculations at the M06/6-311+G(2d,2p):AMBER//B3LYP/6-31G(d,p):AMBER level corresponding to the O_2 addition to C_{18} for all the pathways that have been able to reach the products for snapshots VII and VIII in the aspirin-acetylated COX-2/EPA complex. Antara and supra are the shortening word for antarafacial and suprafacial attack, respectively.

		M06/6-311+G (2d,2p)	
O_2 attack	**Stereochemistry C18 –Snap. VII**	$\Delta E^{\ddagger}$	ΔE
Antara	*S*	4.2	-20.6
Non Supra/Antara	*R*	3.1	-14.7
Non Supra/Antara	*R*	3.1	-14.8
Non Supra/Antara	*R*	2.9	-15.0
Supra	*R*	-0.2	-12.8
O_2 attack	**Stereochemistry C18 –Snap. VIII**	$\Delta E^{\ddagger}$	ΔE
Antara	*S*	2.5	-9.2
Antara	*S*	-1.2	-17.4
Supra	*R*	1.2	-11.9
Supra	*R*	3.6	-15.3